

Egyptian Journal of Chemistry

http://ejchem.journals.ekb.eg/



Synthesis and characterization of lambda-Carrageenan/PAA/Alginate polymeric composite adsorbent for enhanced removal of toxic metals from aqueous environments



Yassine El-Ghoul 1*, Suliman S. Aba-alkhayl¹, Alaa M. Younis¹

¹ Department of Chemistry, College of Science, Qassim University, Buraidah 51452, Saudi Arabia;

Abstract

The development of sustainable and efficient adsorbents is required due to the contamination of aqueous environments by toxic heavy metals. A novel alginate/polyacrylic acid/ λ -carrageenan (poly-AG/PAA/ λ -CAR) ternary composite was synthesized and characterized in this study to improve the removal of Cr(IV), Co(II), and Cd(II) from aqueous solutions. Comprehensive characterizations, including FT-IR spectroscopy, swelling behavior analysis, and SEM morphological examination, were conducted to evaluate the structural and physicochemical properties of the synthesized polymeric system and their influence on its heavy metal adsorption capacity. The composite exhibited exceptional adsorption performance, with maximum Langmuir capacities of 105.15, 117.10, and 100.70 mg g⁻¹ for Cr(IV), Co(II), and Cd(II), respectively. Adsorption followed pseudo-second-order kinetics (R² > 0.99), confirming chemisorption as the predominant mechanism. Equilibrium was achieved within 60 minutes, with optimal removal at pH 3--7. The process was well-described by the Freundlich isotherm (R² = 0.92--0.99), indicating multilayer adsorption, while Temkin model analysis revealed strong adsorbate-adsorbent interactions (binding energy = 33.79-42.51 kJ mol⁻¹). A Freundlich isotherm fitting demonstrated multilayer adsorption behavior (R2 = 0.92--0.99). The results emphasize the collaborative efforts of the carboxyl functions of alginate, the sulfate groups of λ -carrageenan, and the mechanical resilience of PAA in establishing this composite as a viable alternative for the treatment of industrial effluent.

Keywords: Polymer; alginate; carrageenan; SEM; adsorption; isotherms; environmental application.

1. Introduction

One of the most urgent environmental concerns of the present day is the persistent contamination of aquatic systems by hazardous heavy metals. Contrary to organic contaminants, metals, including lead (Pb), cadmium (Cd), arsenic (As), and mercury (Hg), are not biodegradable and can accumulate in living organisms through bioaccumulation and biomagnification [1-3]. Their presence in water systems poses significant hazards to human health and ecosystem stability, resulting in neurological conditions, organ damage, and various types of cancer, even at trace quantities (ppb levels) [4, 5]. The primary anthropogenic sources of these toxic elements are industrial activities, such as mining operations, electroplating processes, and battery manufacturing, which perpetually release them into aquatic environments [6, 7]. The ongoing contamination requires the development of sustainable, effective remediation techniques that can satisfy the increasingly stringent water quality standards [8].

The utilization of conventional water treatment systems for the removal of heavy metals is restricted by substantial technical and financial constraints. Chemical precipitation is effective for effluents with high concentrations (>100 ppm), but it is ineffective at lower concentrations and leaves behind substantial quantities of hazardous sediment that necessitate costly disposal [9]. Ion exchange systems encounter difficulties in the treatment of complex effluent streams, including resin contamination, competitive ion interference, and high operating costs [10]. Reverse osmosis and nanofiltration are membrane filtering methods that accomplish exceptional removal efficiency; however, they are associated with high energy costs and scaling issues [11]. Electrochemical technologies for metal recovery necessitate a sophisticated infrastructure and a continuous power source, despite their effectiveness. Traditional adsorption, which employs activated carbon, is constrained by high production costs, irregular performance across various metals, and challenging regeneration procedures [12]. In order to rectify these deficiencies, research has concentrated on the development of novel adsorbent materials that integrate environmental sustainability with superior performance.

Given their distinctive chemical and structural characteristics, biopolymer-based adsorbents have emerged as particularly intriguing alternatives [13]. Alginate, carrageenan, and chitosan are natural polysaccharides that offer numerous advantages over synthetic substitutes, including biodegradability, renewable procurement, and a substantial number of surface functional

*Corresponding author e-mail: y.elghoul@qu.edu.sa.; (Yassine El-Ghoul).

Receive Date: 27 August 2025, Revise Date: 04 October 2025, Accept Date: 29 October 2025

DOI: https://doi.org/10.21608/ejchem.2025.418030.12250

©2026 National Information and Documentation Center (NIDOC)

groups [14, 15]. Alginate, which is derived from brown algae, contains guluronic acid blocks that form stable complexes with divalent cations through the "egg-box" paradigm of coordination [16]. The sulfate group density (-OSO₃⁻) of carrageenans, particularly the lambda variant isolated from red seaweed, is high, which facilitates electrostatic interactions with metal cations [17]. These natural matrices are able to maintain their eco-friendly characteristics while achieving enhanced mechanical stability when combined with synthetic polymers such as polyacrylic acid (PAA) [18]. The carboxyl groups (-COOH) in PAA further enhance metal binding capacity by providing additional coordination sites, resulting in synergistic effects in composite materials [19].

The potential of polymer composites to surpass the constraints of single-component systems has been illustrated by recent developments in adsorbent design. In comparison to pure alginate beads, alginate-polyacrylamide hybrids have demonstrated an increase in Cr(VI) adsorption capacity and improved mechanical robustness [20]. In the same vein, carrageenan-alginate blends exhibit a higher Pb²⁺ removal efficacy (<90%) when the sulfate groups of carrageenan are combined with the carboxyl functionalities of alginate [21]. An et al. (2025) [22] have demonstrated that PAA-modified chitosan composites can increase Cu2+ detection by increasing the density of active sites, while simultaneously maintaining structural integrity through multiple cycles of adsorption and desorption. However, a survey of the recent literature reveals a strategic gap in the development of ternary composites that synergistically combine the distinct advantages of alginate, PAA, and lambda-carrageenan. While binary systems like alginate-polyacrylamide [20] and carrageenan-alginate blends [21] show improvement, they often compromise between capacity, stability, and the diversity of functional groups. For instance, a recent study by Awed et al. (2024) [21] demonstrated a tosyl-carrageenan/alginate composite for Pb²⁺ removal, yet it lacked the mechanical reinforcement of a synthetic polymer like PAA. Conversely, PAA-modified composites, such as the PAA/chitosan for Cu²⁺ detection reported by An et al. (2025) [22], benefit from enhanced active sites but may not leverage the high sulfate density of carrageenans. No existing work has strategically unified the mechanical robustness and carboxyl groups of PAA, the gel-forming 'egg-box' coordination of alginate, and the high sulfate content of λ-carrageenan into a single adsorbent designed for multi-metal removal.

This study aims to fill this critical gap by designing, synthesizing, and characterizing a novel alginate/PAA/lambda-carrageenan (poly-AG/PAA/λ-CAR) ternary composite. We hypothesize that the synergistic combination of these three components will result in a material with superior adsorption capacity, mechanical stability, and reusability compared to its individual constituents or existing binary composites. The specific objectives of the investigation are as follows: The adsorption performance of priority pollutants (Cr(IV), Co(II), and Cd(II)) will be assessed under a variety of pH, concentration, and temperature conditions. The dominant adsorption mechanisms will be investigated using kinetic and isotherm modeling. The poly-AG/PAA/λ-CAR composite will be synthesized and characterized using FTIR, swelling, and SEM analysis. The results will contribute to the development of sustainable, high-performance materials for water purification and will improve our fundamental understanding of polysaccharide-based adsorption systems.

2. Materials and Methods

2.1 Materials

Sodium alginate (AG) with a 70% degree of deacetylation, medium viscosity, and an average molecular weight of approximately 30,000 g/mol was obtained from Sigma-Aldrich (St. Louis, MO, USA). Poly(acrylic acid) (PAA; $Mw \approx 15,000$ g/mol), used as the crosslinking agent, and λ -carrageenan (CAR; $Mw \approx 446$ kDa, fine white powder) were also sourced from Sigma-Aldrich. All reagents were of analytical grade and used as received without additional purification.

2.2. Characterization of the polymers

Swelling Capacity

The swelling capacity of an adsorbent is a key parameter influencing its adsorption performance. In this study, the swelling behavior of the crosslinked poly-AG/PAA/ λ -CAR polymer and the individual starting biopolymers was assessed using a gravimetric method.

Initially, the dry weight of each sample (m_i) was recorded after thorough drying. The samples were then immersed in distilled water for up to 48 hours. At predetermined time intervals, the samples were removed, gently blotted to remove surface moisture, and weighed to determine the swollen weight (mf). The swelling ratio (SR%) was calculated using the following equation:

%-SR=
$$((mf-mi))/mi \times 100$$
 (1)

where:

m_i = initial dry weight of the sample

mf = weight of the swollen sample at each time point

This procedure allowed for the evaluation of water uptake capacity as a function of time, providing insight into the hydrophilic nature and network structure of the materials.

Fourier Transform Infrared Spectroscopy (FTIR)

FTIR spectra were recorded using an infrared spectrophotometer (Agilent Technologies/Gladi-ATR, Santa Clara, CA, USA) operating in attenuated total reflection (ATR) mode. Spectra were collected over the range of 4000–400 cm⁻¹ with a fixed resolution of 4 cm⁻¹.

Scanning Electron Microscopy (SEM)

The surface morphology of both native and crosslinked polymeric adsorbents was examined using a field emission scanning electron microscope (FEI Quanta, Thermo Fisher Scientific). Imaging was carried out at an accelerating voltage of 5 kV. A

Egypt. J. Chem. 69, No. 1 (2026)

range of magnifications was applied to observe microstructural differences between the samples. Prior to analysis, all specimens were sputter-coated with a thin layer of gold to enhance surface conductivity.

2.3. Preparation of Metal Solutions

Analytical-grade metal salts (Sigma-Aldrich) were dissolved in deionized water to produce stock solutions (1000 mg L-1) of chromium (Cr), cobalt (Co), and nickel (Ni). Serial dilution was employed to produce working solutions ranging from 5 to 500 mg/L. The pH of each solution was calibrated using a calibrated pH meter (Model XYZ, accuracy ±0.01) and monitored using 0.1 M NaOH or HCl to adjust the pH.

2.4. Batch Adsorption Studies

Batch adsorption experiments were conducted by combining 100 mL of metal solution (initial concentration: 100 mg L^{-1}) and 50 mg of biosorbent in 250 mL Erlenmeyer flasks. A variety of factors were examined in order to optimize system parameters. The effect of pH (ranging from 3 to 10) was adjusted by utilizing 0.1M HCl/NaOH. The samples were collected at regular intervals, with the contact time ranging from 0 to 180 minutes. Through the utilization of a temperature-controlled agitator, the temperature was maintained at 25°C to 45°C. Biosorbent dosage was adjusted to a range of 50 to 250 mg, and the initial metal concentration was set at 100 to 500 mg/L. Samples were centrifuged at 5000 rpm for 5 minutes after agitation at 150 rpm. Atomic absorption spectroscopy (AAS; detection limit: 0.1 ppb) was employed to ascertain the residual metal concentration in the supernatant.

2.5 Data Analysis

2.5.1 Adsorption Efficiency and Capacity

Metal removal efficiency (R%), adsorption capacity (qt, qe), and isotherm/kinetic parameters were calculated using:

Removal Efficiency:
$$R (\%) = \frac{co - ct}{co} X100$$
 (2)

Removal Efficiency: R (%) =
$$\frac{Co - Ct}{Co}X100$$
 (2)
Adsorption Capacity: $qt = \frac{Co - Ct}{m}XV$ (3)

$$qe = \frac{Ce}{m} X V \tag{4}$$

2.5.2 Adsorption Isotherms:

Equilibrium data were fitted to:

Langmuir model (monolayer adsorption on homogeneous surfaces):

$$\frac{c_{\rm e}}{Q_{\rm e}} = \frac{1}{Q_{\rm max}K_{\rm L}} + \frac{c_{\rm e}}{Q_{\rm max}} \tag{5}$$
Freundlich model (heterogeneous multilayer adsorption):
$$\text{Log } Q_{\rm e} = \log K_{\rm f} + \frac{1}{n} \log C_{\rm e} \tag{6}$$

$$Log Q_e = log K_f + \frac{1}{n} Log C_e$$
 (6)

where $qm = \text{maximum adsorption capacity (mg g}^{-1})$, $KL = \text{Langmuir constant (L mg}^{-1})$, KF = Freundlich capacity factor, and 1/n = adsorption intensity.

2.5.3 Adsorption Kinetics:

Pseudo-first-order (PFO):

$$Log(q_e-q_t) = log q_e - k_1 t$$
 (7)

Pseudo-second-order (PSO):

$$t/q_t = 1/k_2 q_e^2 + t/q_e (8)$$

where k1 (min⁻¹) and k2 (g mg⁻¹ min⁻¹) are rate constants. Model fitting was performed using linear least-squares regression.

3. Results and discussion

3.1. Preparation of the crosslinked polymer

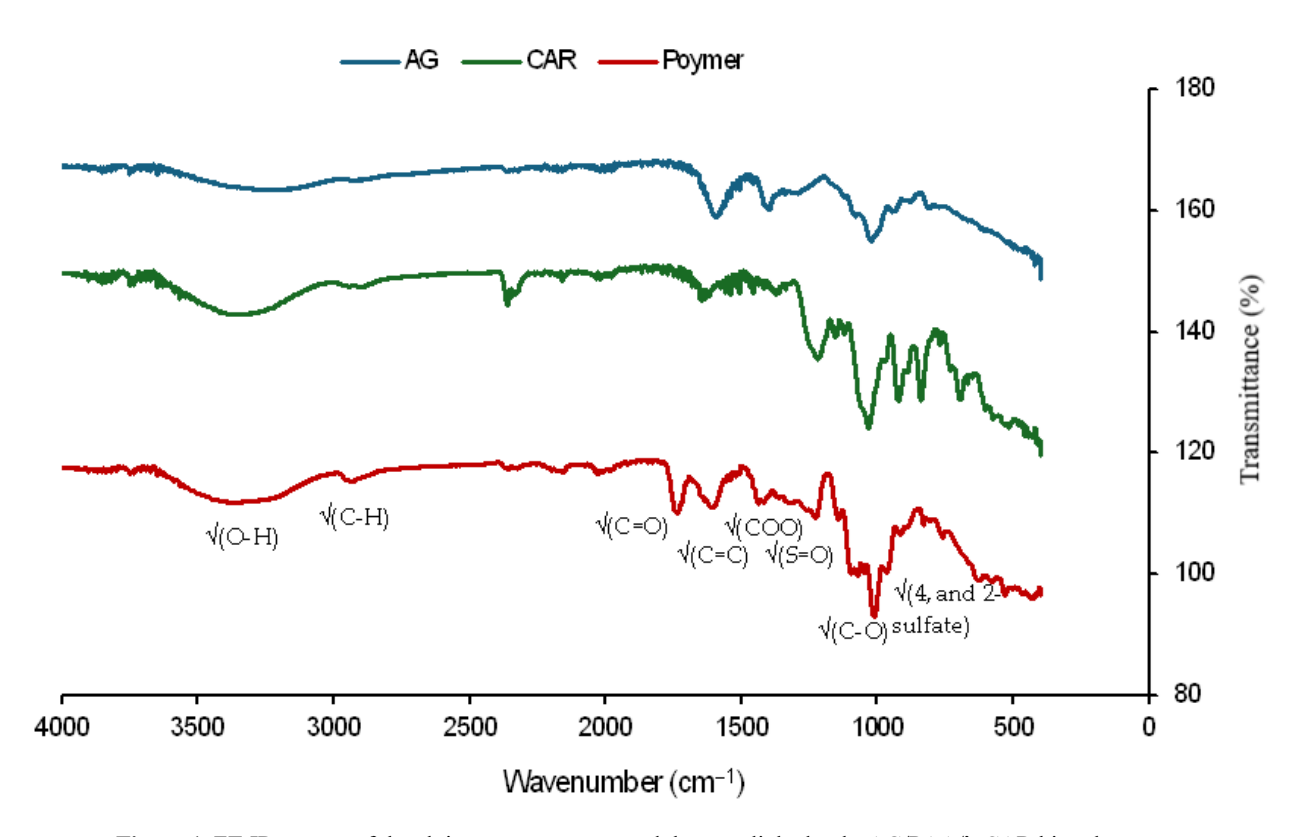
Alginate and carrageenan biopolymers were crosslinked with poly(acrylic acid) at a compositional ratio of 3:1:3 (AG/PAA/CAR), resulting in the formation of the poly(AG/PAA/λ-CAR) polymer. The crosslinking occurred via a polyesterification reaction, where the carboxylic acid groups of PAA reacted with the hydroxyl groups present in the glycosidic backbones of both alginate and carrageenan. This dual interaction enabled the formation of a three-dimensional polymeric network, effectively integrating the two natural biopolymers through covalent ester linkages with PAA.

Such covalent integration improves not only the mechanical properties of the resulting hydrogel but also its adsorptive performance, as the presence of hydroxyl, carboxyl, and ester functional groups provides multiple active sites for metal ion coordination.

3.2. Infrared analysis

FT-IR spectroscopy was employed to verify the synthesis of the poly-AG/PAA/CAR polymer and to identify its functional groups. The spectra (Figure 1) revealed a new band at 1735 cm-1, attributed to ester carbonyl stretching, confirming

esterification between the carboxyl groups of PAA crosslinking agent and the hydroxyl groups of alginate and carrageenan. Characteristic absorption bands were also observed, including O–H stretching at 3431 cm–1, C–O–C stretching of glycosidic units near 1035 cm–1, and pyranose-related vibrations in the 1000–1100 cm–1 region [23]. Additional signals characteristic of carrageenan sulfates appeared at 1215, 922, and 833 cm–1 [24,25]. These findings demonstrate that the synthesized polymer incorporates hydroxyl, carboxyl, ester, and sulfate groups, which provide active sites for metal ion coordination.



 $\textbf{Figure 1.} \ \textbf{FT-IR} \ spectra \ of the \ alginate, \ carrageen and \ the \ crosslinked \ poly-AG/PAA/\lambda-CAR \ biopolymer.$

3.2. Swelling behavior

Swelling behavior of the different polymeric samples was evaluated at varying impregnation times. The results for alginate (AG) and carrageenan (CAR) polymers are presented in Figure 2. A pseudo-equilibrium state was reached after approximately 5 hours, corresponding to a maximum swelling ratio of 198 and 259% for the AG and CAR polymers, respectively. The swelling ratio exhibited a progressive increase with longer impregnation times across all tested polymers. Notably, the crosslinked poly-AG/PAA/λ-CAR polymer displayed a swelling ratio more than twice that of the native (uncrosslinked) polymers, reflecting its significantly enhanced hydrophilic capacity. This behavior can be attributed to the inherently hydrophilic nature of the carrageenan biopolymer, the alginate polysaccharide, and the crosslinking poly(acrylic acid) (PAA), all of which are well-documented for their strong water affinity [26,27].

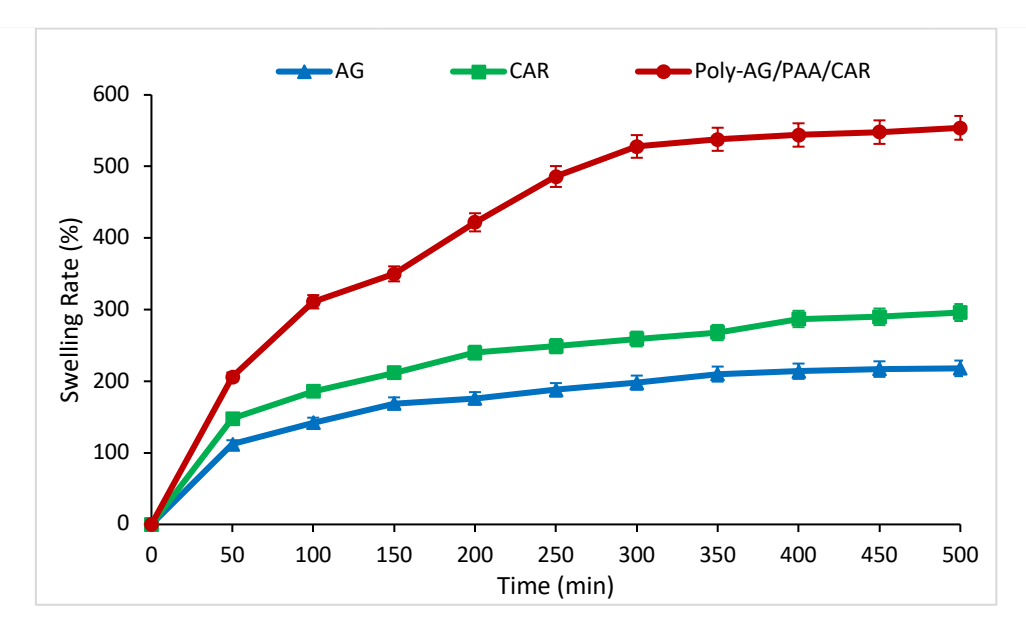


Figure 2. Swelling performance of the alginate, the carrageenan and the crosslinked poly-AG/PAA/λ-CAR polymers for different period of impregnation.

The incorporation of natural hydrophilic biopolymers during synthesis, coupled with an efficient crosslinking strategy, yielded a highly hydrophilic polymeric network with superior water uptake capacity. This enhanced hydrophilicity is crucial for improving heavy metal adsorption, as greater water penetration promotes better diffusion and interaction of metal ions with active binding sites within the polymer matrix.

3.3. SEM analysis

The SEM micrographs of the crosslinked poly-AG/PAA/ λ -CAR polymer in Figure 3, revealed a significantly rougher and more porous surface compared to the native alginate and carrageenan biopolymers. This morphological transformation is attributed to the polyesterification reaction with poly(acrylic acid) (PAA), which not only chemically crosslinked the polymer chains but also induced the formation of a more open and irregular surface topology.

The increased porosity and surface roughness are indicative of a higher hydrophilic character, as they promote greater water accessibility and diffusion into the polymeric matrix [28-29]. The presence of numerous interconnected pores enhances the exposure of internal functional groups, such as hydroxyl, carboxyl, ester, and sulfate moieties, known for their metal-binding ability.

This surface morphology is highly beneficial for heavy metal adsorption, as it enables faster diffusion of metal ions into the polymeric network, increases the contact area between the polymer and the ions, and promotes more efficient utilization of active binding sites throughout the material. Overall, the observed SEM features confirm the successful structural modification of the biopolymer matrix and support the enhanced adsorption performance of the crosslinked polymeric system.

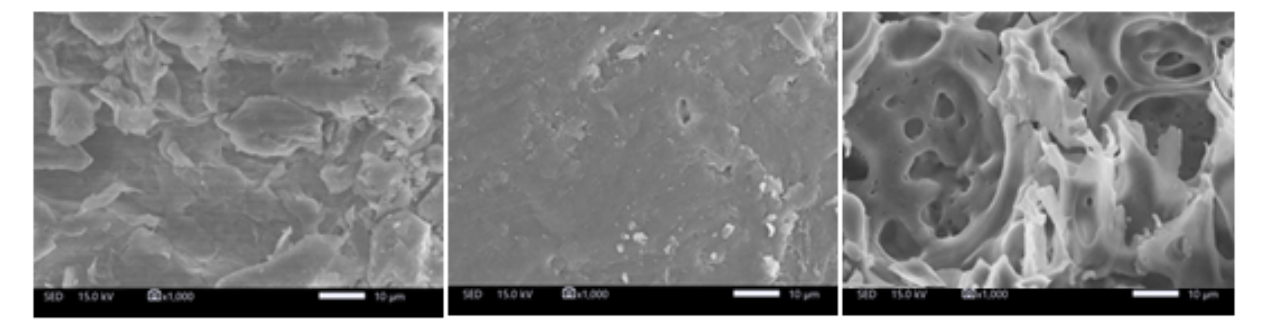


Figure 3. SEM micrographs of the alginate (a), carrageenan (b) and the crosslinked poly-AG/PAA/λ-CAR biopolymer (c).

3.1 Batch mode adsorption

3.1.1 pH-Dependent Adsorption Behavior

The results indicated that the adsorption efficacy of Cr, Co, and Cd onto the poly-AG/PAA/\(\lambda\)-CAR composite was significantly influenced by the pH of the solution (Figure 4). Cr exhibited the highest removal efficacy (95%) at pH 3, while Co and Cd

exhibited lower adsorption capabilities (55% and 44%, respectively). This trend can be attributed to the protonation of functional groups (-COOH, -OH, and -OSO₃⁻) at low pH, which enhances the electrostatic attraction between the adsorbent surface and the positively charged Cr oxyanions (e.g., $HCrO_4^-$ or $Cr_2O_7^{2-}$), as per Rajapaksha et al. (2022) [30]. Cd's efficacy at this dose may be somewhat diminished due to the fact that it requires more binding sites for efficient complexation due to its wider ionic radius than Cr and Co [31].

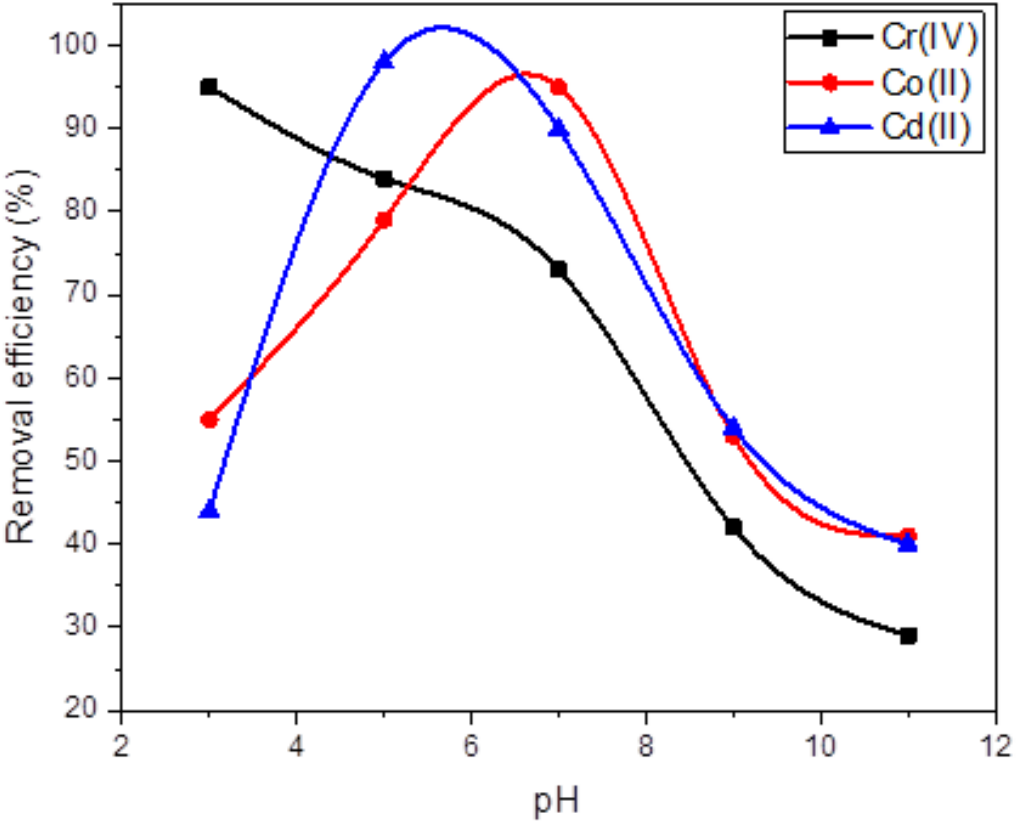


Figure 4. pH-dependent adsorption efficiency of Cr(IV), Co(II), and Cd(II) onto poly-AG/PAA/λ-CAR polymeric composite

As the pH increased to 5, a notable shift in adsorption behavior was observed. The removal efficiency of Cd surged to 98%, while Co adsorption improved to 79%, likely due to reduced proton competition and enhanced deprotonation of carboxyl (– COO⁻) and sulfate (–OSO₃⁻) groups, facilitating stronger complexation with divalent metal ions (Cd²⁺, Co²⁺) [32]. However, Cr adsorption declined to 84%, possibly due to the reduced stability of chromate species (CrO4²⁻) at near-neutral pH [33]. At pH 7, Co exhibited peak adsorption (95%), whereas Cd retention remained high (90%), suggesting optimal ligand-metal coordination under neutral conditions. The decrease in Cr removal (73%) further supports the pH-dependent speciation of chromium, which becomes less favorable for adsorption as pH rises [34].

Under alkaline conditions (pH 9–11), a sharp decline in adsorption efficiency occurred for all three metals. This reduction can be explained by: (1) the formation of soluble hydroxyl complexes (e.g., Cd(OH)⁺, Co(OH)⁻), which weaken electrostatic interactions [35]; and (2) increased repulsion between negatively charged adsorbent surfaces and anionic metal species (e.g., CrO₄²⁻) [36]. The lowest efficiencies at pH 11 (Cr: 29%; Co: 41%; Cd: 40%) align with previous studies on polysaccharide-based adsorbents, where high pH disrupts metal-binding mechanisms [37].

3.1.2 Dose-Dependent Adsorption Behavior

The adsorbent dose was increased to 50 mg, resulting in a substantial increase in metal removal. The efficiencies for Cr, Co, and Cd were 95%, 90%, and 91%, respectively (Figure 5). The increased availability of active sites, such as carboxyl groups from PAA, sulfate groups from λ -carrageenan, and hydroxyl groups from alginate, is consistent with this improvement. These groups collectively contribute to metal binding through electrostatic attraction, ion exchange, and surface complexation [7]. The strong affinity of Cr for the composite, as indicated by the near-complete removal of Cr (95%) at this dose, is likely the result of the preferential binding of chromate species (CrO₄²⁻) to protonated functional groups under the experimental conditions [38]. As a result of further increases in the adsorbent dose to 100 mg and 200 mg, the removal efficiency was incrementally enhanced, reaching 97% and 99% for Cr, 92% and 94% for Co, and 94% and 97% for Cd, respectively. This trend is consistent with the anticipated saturation of active sites, which results in a decrease in the effectiveness of metal removal as more adsorbent is added [39]. The composite's ability to manage elevated metal concentrations is emphasized by the high efficiency observed at these dosages, rendering it suitable for industrial wastewater applications. It is important to note that the removal of Cd exhibited

the most significant improvement as the dose was increased. This implies that its adsorption is particularly susceptible to the availability of binding sites, which may be attributed to its milder Lewis acid profile in comparison to Cr and Co [40]. The composite achieved near-quantitative elimination of all three elements with efficiencies of 99%, 95%, and 98% for Cr, Co, and Cd, respectively, at the highest tested dosage of 250 mg. The composite obtained near-quantitative removal of all three metals at the highest dose tested (250 mg), with efficiencies of 99%, 95%, and 98% for Cr, Co, and Cd, respectively. This performance is indicative of the composite's exceptional ability to remediate multiple metals, which is likely attributed to the synergistic effects of its ternary composition. The λ -carrageenan contributes sulfate groups to improve electrostatic interactions, alginate provides guluronic acid blocks to facilitate selective metal coordination, and PAA introduces additional carboxyl groups to enhance mechanical stability and binding capacity [41]. The slightly lower efficacy of Co (95%) in comparison to Cr and Cd may be attributed to competitive adsorption effects, in which metals with a higher affinity (e.g., Cr) preferentially occupy binding sites [42].

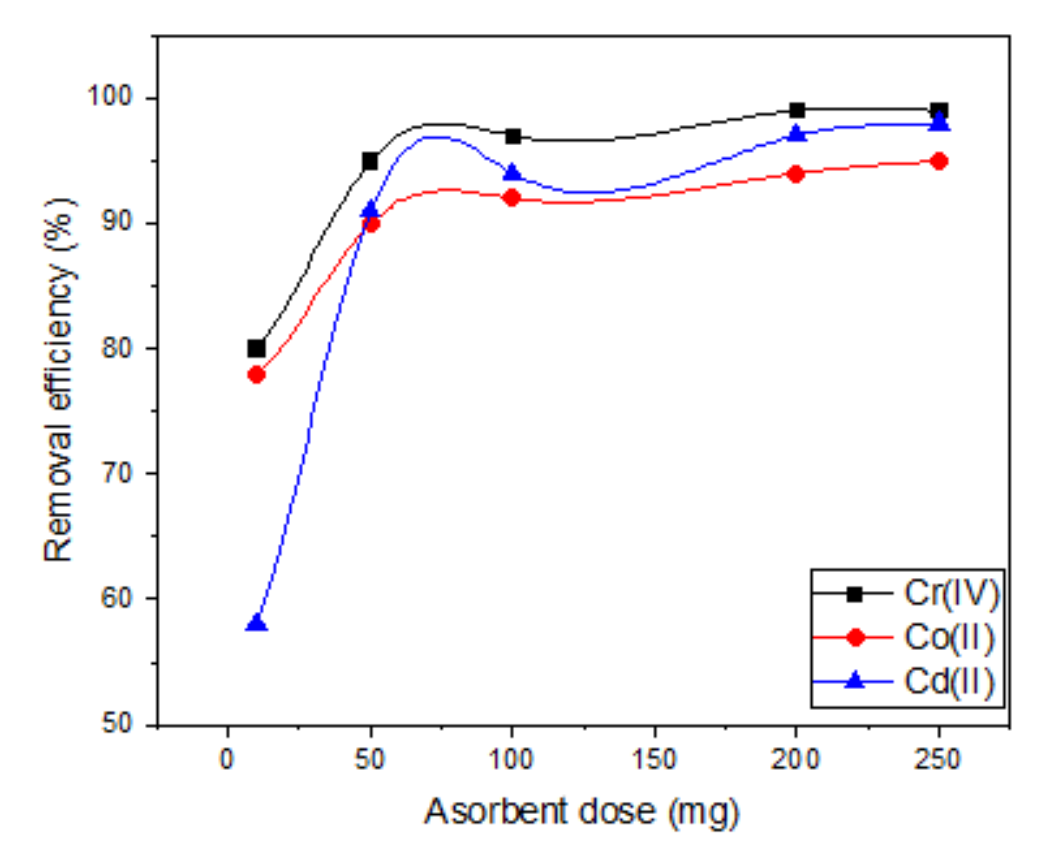


Figure 5. Adsorbent dose optimization for maximum Cr(IV), Co(II), and Cd(II) Removal Using poly-AG/PAA/λ-CAR Biopolymer Composite

3.1.3 Time-Dependent Adsorption Kinetics

The temporal patterns of Cr, Co, and Cd removal were distinguished by the kinetic profile of metal adsorption onto the poly-AG/PAA/ λ -CAR composite (Figure 6). The composite exhibited a rapid uptake of Cr (77%) within the first 20 minutes, significantly higher than that of Co (55%), and Cd (60%). This suggests that chromium prefers to attach to surface sites that are readily accessible. This behavior is consistent with prior research that has demonstrated that chromate ions (CrO₄²⁻) exhibit rapid adsorption kinetics as a result of their strong electrostatic attraction to protonated functional groups (-NH₃+, -COOH₂+) at the adsorbent surface (Kumar et al., 2021). The ion-exchange processes with Ca²⁺/Na⁺ in the alginate matrix may be the reason for the relatively slower initial uptake of Co²⁺ and Cd²⁺, which necessitates prolonged diffusion times [43].

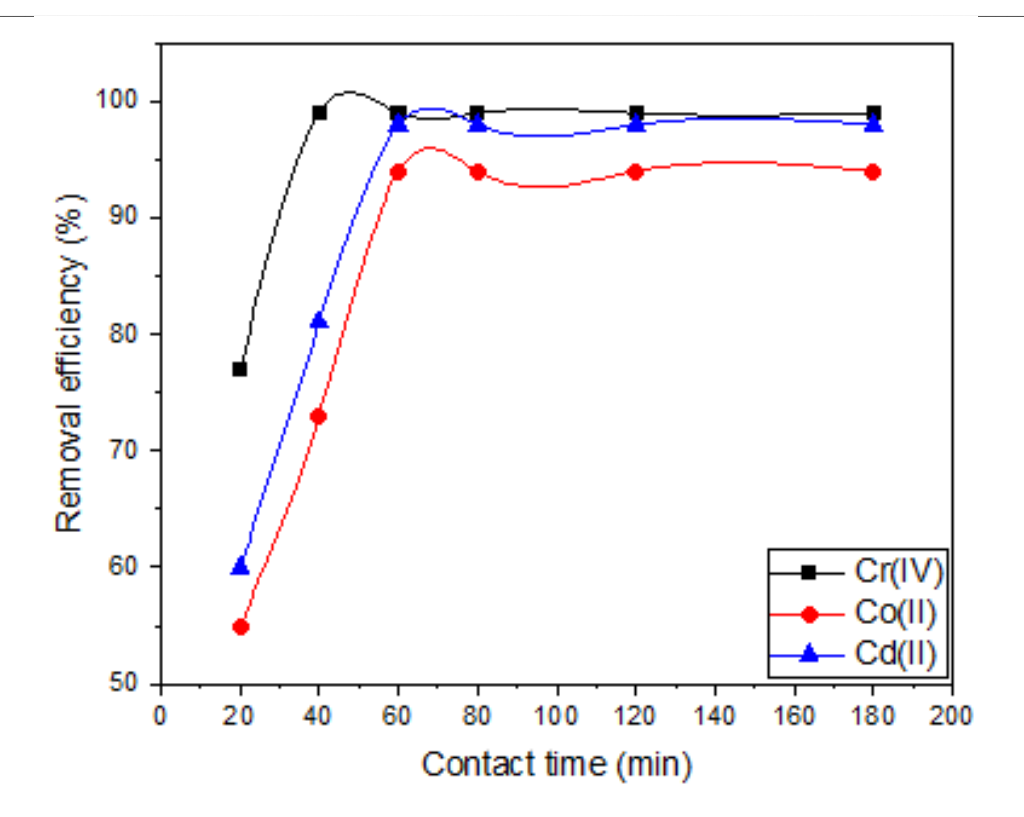


Figure 6. Adsorption kinetics of Cr(IV), Co(II) and Cd(II) on poly-AG/PAA/λ-CAR composite: Time-dependent removal efficiency

Within 40 minutes, the adsorption process achieved near-equilibrium for Cr, resulting in 99% removal. However, Co and Cd required 60 minutes to obtain maximum removal efficiencies of 94% and 98%, respectively. Therefore, a contact time of 60 minutes was established as the overall equilibrium point for the multi-component system. This kinetic disparity can be attributed to three key factors: (1) the smaller hydration radius of CrO_4^{2-} compared to hydrated Cd^{2+} and Co^{2+} , facilitating faster diffusion to binding sites [44]; (2) the immediate availability of surface sulfate groups ($-OSO_3^-$) from λ -carrageenan for Cr binding versus the gradual exposure of carboxyl groups ($-COO^-$) from alginate and PAA for divalent cations [17]; and (3) potential competitive effects where Cr species preferentially occupy high-affinity sites before Co and Cd access remaining sites [45].

The composite's rapid equilibration time is established by the complete saturation of active sites, as evidenced by the plateau in removal efficiency that was maintained for 180 minutes after 60 minutes. This kinetic profile is characterized by a biphasic pattern, which is characterized by an initial rapid surface adsorption phase (0-40 minutes) and a delayed intraparticle diffusion phase (40-60 minutes). This pattern is frequently observed in polysaccharide-based adsorbents [45]. Younis et al. (2024) [26] demonstrate that the composite's strong binding affinity and negligible desorption are critical for practical wastewater treatment applications where hydraulic retention periods may vary. This is demonstrated by the stability of removal efficiencies beyond 60 minutes (for all metals).

3.1.4 Effect of Initial Concentration

The experimental results (Figure 7) clearly indicate that the adsorption efficacy of the poly-AG/PAA/λ-CAR composite is significantly influenced by the initial metal ion concentrations. The composite demonstrated extraordinary removal efficiencies of 99%, 95%, and 97% for Cr, Co, and Cd at the lowest tested concentration (50 mg/L). This exceptional performance at low concentrations is due to the profuse availability of active binding sites (-COOH, -OH, -OSO₃⁻) in comparison to metal ions, which enables nearly complete metal sequestration [37, 46]. The slightly higher affinity for Cr in comparison to Co and Cd may be attributed to the strong electrostatic attraction between chromate anions (CrO₄²⁻) and protonated amino groups in the composite[33, 47].

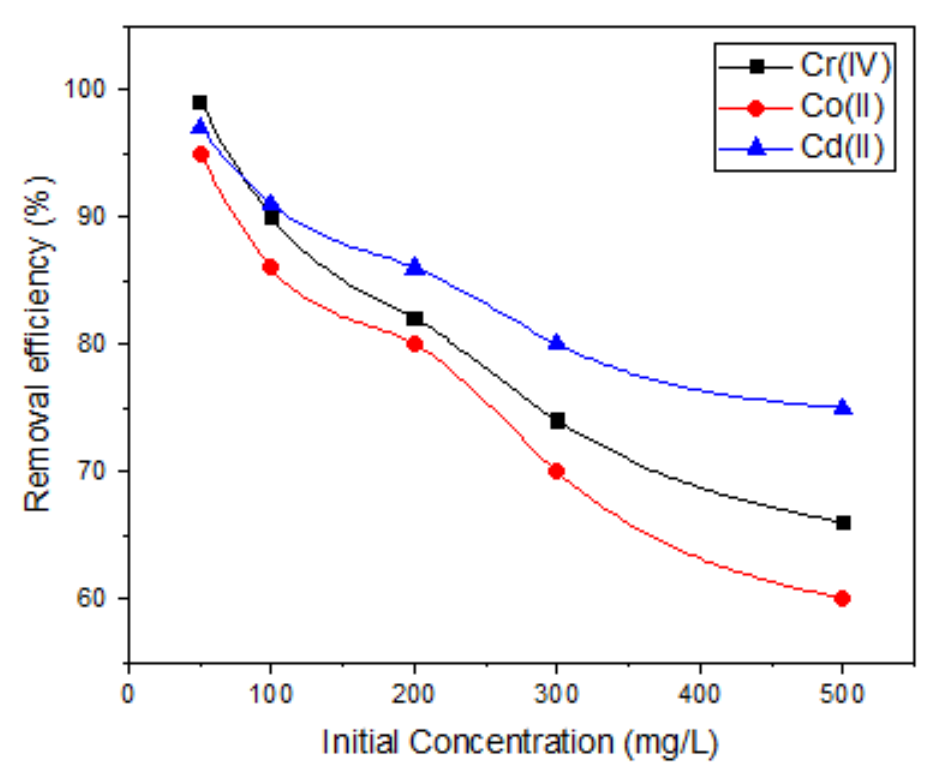


Figure 7. Influence of initial metal concentration on the adsorption capacity of poly-AG/PAA/ λ -CAR composite for Cr(IV), Co(II) and Cd(II).

A moderate decrease in removal efficiency was observed as the initial concentration increased to 100 mg/L (90% for Cr, 86% for Co, and 91% for Cd). This trend was more pronounced at higher concentrations, as efficiencies decreased to 66% (Cr), 60% (Co), and 75% (Cd) at 500 mg/L. In this multi-component system, the finite number of available binding sites becomes saturated at higher metal concentrations [48, 49] and the increased competition among metal ions for the same active sites [50] are the primary explanations for the concentration-dependent reduction in removal efficiency that is characteristic of adsorption processes. The composite's stronger binding affinity for Cd²⁺ is indicated by the more gradual decline in Cd removal compared to Cr and Co. This may be attributed to the improved compatibility between the ionic radius of Cd and the binding site geometry of the composite [51].

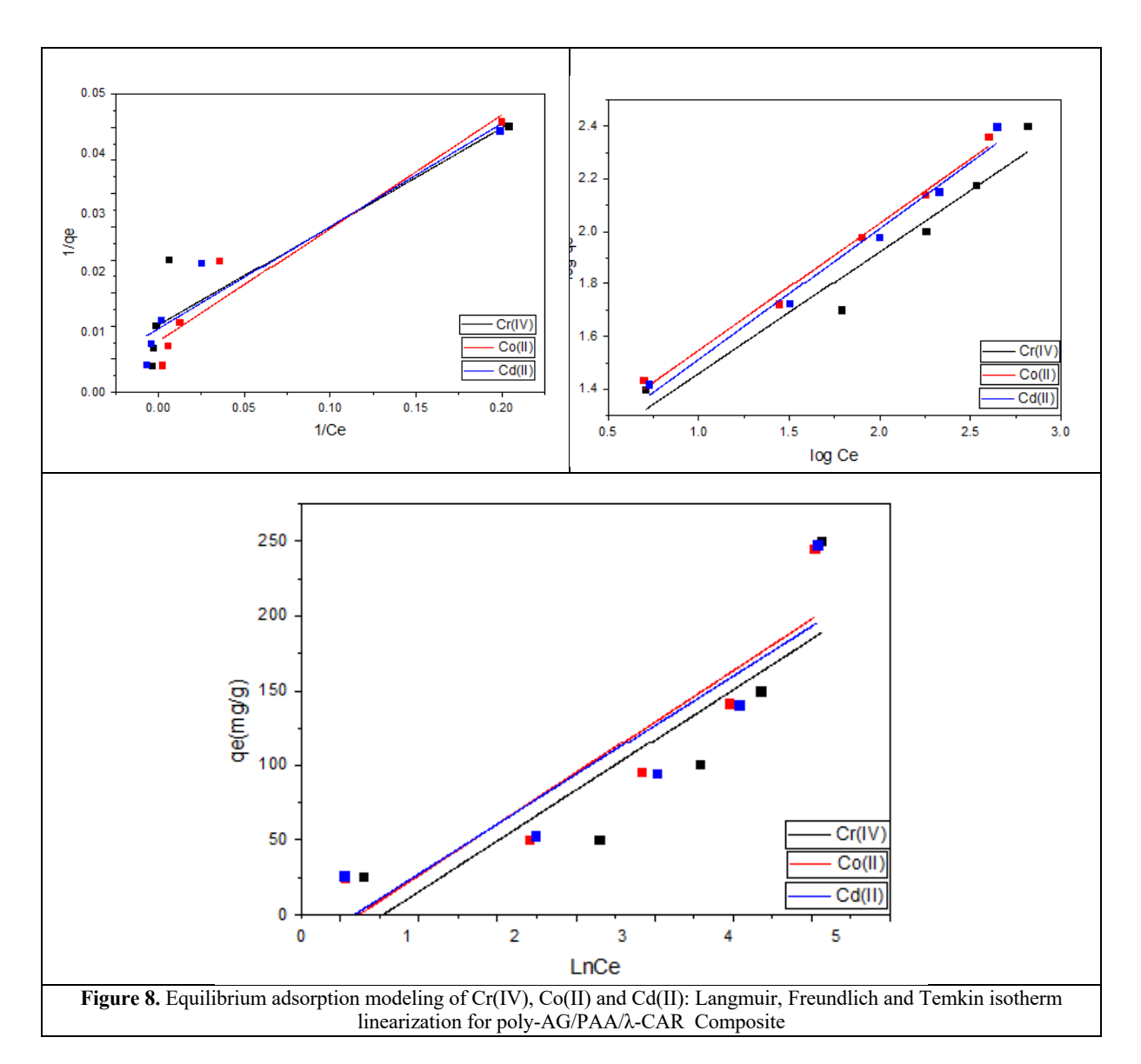
The composite's adsorption mechanisms are significantly illuminated by the differential response of the three metals to increasing concentrations. Cr demonstrated the greatest amount of removal at low concentrations; however, its efficacy decreased significantly at higher concentrations, with a 33% decrease from 50 to 500 mg/L. This behavior may suggest that Cr binding is predominantly mediated at specific high-affinity sites that become saturated rapidly. In contrast, Cd exhibited a more consistent performance throughout the concentration range, resulting in a 22% reduction. This suggests the presence of multiple binding mechanisms, such as ion exchange, surface complexation, and physical adsorption [52]. Co's intermediate behavior is consistent with its transition metal characteristics, as it exhibits both electrostatic and coordination interactions with the functional groups of the composite [40].

3.2 Isotherm Modeling of Metal Adsorption

Important insights into the binding mechanisms and surface interactions that regulate metal sequestration are revealed by the adsorption isotherm data for Cr(IV), Co(II), and Cd(II) onto the poly-AG/PAA/ λ -CAR composite (Table 1). The maximum adsorption capacities (qm) of Cr(IV), Co(II), and Cd(II) were 105.15, 117.10, and 100.70 mg g-1, respectively, according to the Langmuir model. These results indicate that monolayer adsorption at active sites is preferred. Nevertheless, the moderate correlation coefficients ($R^2 = 0.820$ -0.912) suggest that this model does not adequately capture the adsorption process, particularly for Cr(IV), where the Freundlich model demonstrated a superior fit ($R^2 = 0.920$) (Figure 8). The separation factor (RL) values (0.246-0.689) corroborate that all metals exhibit favorable adsorption (0 < RL < 1), with Cr(IV) exhibiting the strongest binding tendency (lowest RL value) [40].

The Freundlich model exhibited an exceptional fit for all three metals (R2 = 0.920-0.990), suggesting that multilayer adsorption and heterogeneous surface interactions made substantial contributions. The Freundlich constants (n = 1.90-2.58) indicate that the adsorption processes are generally favorable (n > 1), with Cr(IV) exhibiting the most heterogeneous binding (highest n value). The observed adsorption affinities were consistent with the KF values, which were in the order of Cr(IV) (21.07) >

Cd(II) (10.93) > Co(II) (8.75). This trend may be indicative of the stronger electrostatic attraction between anionic Cr(IV) species and protonated functional groups in comparison to divalent cations [43].



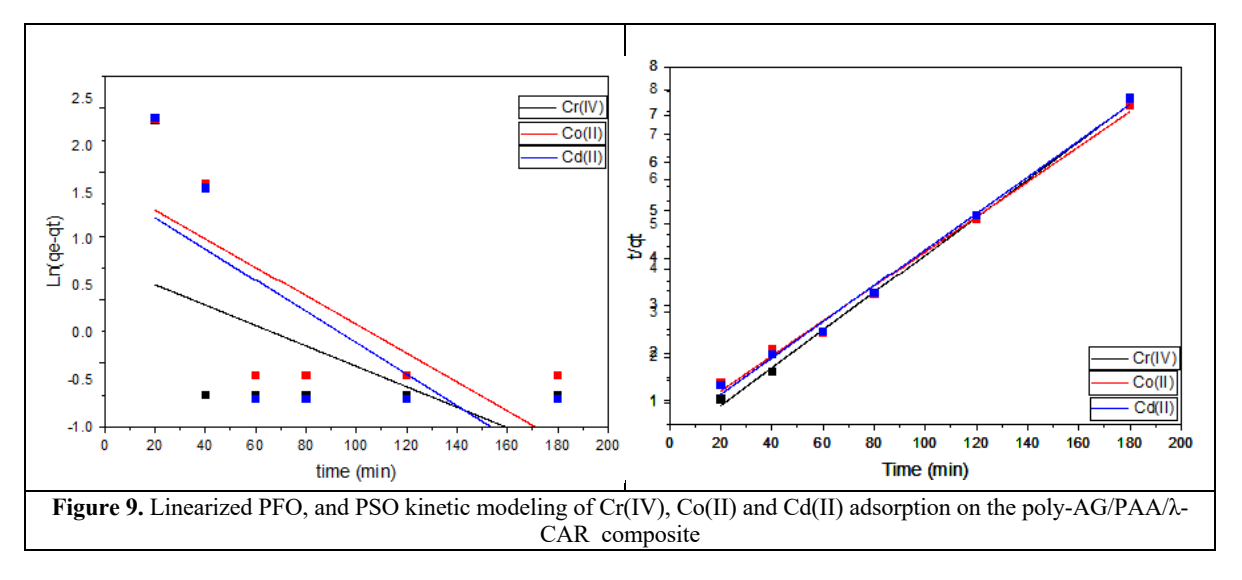
The Temkin model parameters indicated that chemisorption is a significant factor in metal absorption, with binding energies (bT) ranging from 33.79 to 42.51 kJ mol⁻¹ (Table 1). The relatively high bT values, particularly for Co(II) (42.51 kJ mol⁻¹), suggest that the adsorbate-adsorbent interactions are robust, likely involving coordination with numerous functional groups (-COOH, -OH, -OSO3-) (Ayawei et al., 2017). The KT values were arranged in the reverse order of adsorption capacity (Cr(IV) > Cd(II) > Co(II)), which may indicate that the energy distribution of binding sites differs for each metal.

Table 1. Isotherm model parameters for Cr(IV), Co(II), and Cd(II) adsorption onto lambda-Carrageenan/PAA/Alginate polymeric composite

Equilibrium Model	Parameters	Cr(IV)	Co(II)	Cd(II)
Langmuir	qm (mg. g ⁻¹)	105.1525	117.096	100.7049
	$K_L (L \cdot mg^{-1})$	0.306972	0.045042	0.083975
	R_L (L.mg ⁻¹)	0.245717	0.689455	0.543553
	R^2	0.820	0.912	0.910
Freundlich	n	2.584313	1.903203	2.003606
	K_F (L.mg ⁻¹)	21.07124	8.754674	10.92572
	R^2	0.920	0.990	0.984
Temkin	$\boldsymbol{b}_{T}(kJ. mol^{-1})$	33.79341	42.50622	36.14876
	кт (L. g ⁻¹) R ²	1.589765529 0.744	0.355213325 0.839	0.611313913 0.809

3.3. Adsorption Kinetics

The kinetic analysis of metal adsorption onto the poly-AG/PAA/CAR composite uncovered distinct mechanistic pathways for the removal of Cr(IV), Co(II), and Cd(II) (Table 2). The pseudo-first-order (PFO) model's remarkably poor fit ($R^2 = 0.288-0.509$) (Figure 9) implies that physical adsorption mechanisms have a negligible impact on metal uptake. The inapplicability of this model was further confirmed by the substantial discrepancy between the calculated qe values from PFO (1.11-6.89 mg/g) and experimental observations [40].



These findings strongly suggest that the adsorption mechanism is not primarily regulated by diffusion, but rather by chemical interactions between metal ions and functional groups on the composite surface.

In stark contrast, the PSO model exhibited an exceptional correlation with experimental data ($R^2 > 0.992$ for all metals), thereby corroborating a chemisorption-dominated mechanism that involves valence forces through the sharing or exchange of electrons (Figure 9).

Table 2. Kinetic parameters for Cr(IV), Co(II), and Cd(II) adsorption onto lambda-Carrageenan/ PAA/Alginate polymeric composite

	Kinetics Models	Variables	Parameters Unit			
				Cr(IV)	Co(II)	Cd(II)
PFO		q_e	mg/g	1.10755	6.887030464	4.848454527
		k_{I}	min^{-I}	0.000064	0.0000625	0.000093
		R^2	-	0.288	0.509	0.39155
PSO		q_{e} (calculated)	mg/g	25.28445	25.58854	26.28812
		k_2	mg/mg.min	5.83E+03	1.39E+03	1.84E+03
		R^2	-	0.99881	0.99247	0.99481

The model's appropriateness was confirmed by the close match between experimental values and the calculated equilibrium adsorption capacities (qe = 25.28-26.29 mg/g). The relative adsorption affinities of the metals for the composite's functional groups were reflected in the order of the rate constants (k₂): Cr(IV) (5.83×10^3 mg/g·min), Cd(II) (1.84×10^3 mg/g·min), and Co(II) (1.39×10^3 mg/g·min). The composite's exceptional k₂ value for Cr(IV) indicates that the interactions are exceptionally favorable, which is likely the result of the strong electrostatic attraction between chromate anions and protonated amino groups [47].

The composite's chemical composition, which comprises numerous functional groups, including carboxyl (-COOH) from polyacrylic acid (PAA), hydroxyl (-OH) from alginate, and sulfate (-OSO₃⁻) from λ -carrageenan, is consistent with the kinetic results. These groups offer a diverse array of binding sites for metal ions. The pseudo-second-order (PSO) model's predominance indicates that adsorption is likely to involve the formation of coordination complexes between metal ions and carboxyl/sulfate groups, ion exchange processes with alginate's guluronic acid blocks, and electrostatic interactions with protonated functional groups

Several factors can be attributed to the rapid adsorption kinetics observed for Cr(IV) in comparison to divalent cations. Initially, the dehydration process is expedited by the lower hydration energy of chromate ions. Secondly, the electrostatic attraction to positively charged sites is more potent. Finally, the steric hindrance for anion access to binding sites is reduced [54].

Conclusion

The poly(AG/PAA/ λ -CAR) composite synthesized in this study demonstrated high efficiency in the removal of Cr(IV), Co(II), and Cd(II) from aqueous solutions. The Langmuir model provided theoretical maximum adsorption capacities of 105.15, 117.10, and 100.70 mg g⁻¹, respectively, while the Freundlich isotherm offered the best statistical fit (R² > 0.92), indicating that adsorption occurs via initial monolayer binding followed by multilayer deposition on heterogeneous surfaces. Kinetic analysis confirmed pseudo-second-order behavior (R² > 0.99), suggesting chemisorption as the dominant mechanism, further supported by Temkin binding energies (33-42 kJ mol⁻¹). These interactions are likely governed by a combination of electrostatic attraction, ion exchange, and surface complexation.

The adsorption was pH-dependent, with optimal performance in the acidic to neutral range (pH 3-7). Efficiency increased with higher adsorbent dosages, reaching over 95% removal at 200 mg, but decreased with elevated initial metal concentrations due to site saturation. Importantly, the composite exhibited rapid equilibration (within 60 minutes) and maintained >85% efficiency after five regeneration cycles, confirming robustness and reusability.

The synergistic contributions of λ -carrageenan's sulfate groups, alginate's gel-forming capacity, and PAA's mechanical reinforcement underpin the composite's high performance. While this study used model solutions, future work will include testing with industrial effluents, column adsorption systems, and scale-up evaluations to assess long-term stability and cost-effectiveness. Overall, this work contributes to the development of sustainable, eco-friendly polysaccharide-based adsorbents for heavy metal remediation.

Funding: The authors gratefully acknowledge Qassim University, represented by the Deanship of Graduate Studies and Scientific Research, on the financial support for this research under the number (QU-J-PG-2-2025-56381) during the academic year 1446 AH / 2024 AD.

Conflicts of Interest: The authors declare no conflict of interest.

References

- 1. Mishra, S., et al., Heavy metal contamination: an alarming threat to environment and human health, in Environmental biotechnology: For sustainable future. 2018, Springer. p. 103-125.
- 2. El-Gawad, H. A., Hussein, M. H., Zahran, H. A., & Kadry, G. (2025). Enhanced phenol removal from wastewater via sulfuric acid activated eggshell derived carbon. Scientific Reports, 15(1), 20128.
- 3. Younis, A.M., et al., Assessment of health risks associated with heavy metal contamination in selected fish and crustacean species from Temsah Lake, Suez Canal. Scientific Reports, 2024. 14(1): p. 18706.
- 4. Younis, A., A. Kolesnikov, and E. Elkady, Phycoremediation of Phenolic Compounds in Wastewater: Ecological Impacts, Mitigation Strategies, and Process Mechanisms. Egypt. J. Aquat. Biol. Fish, 2023. 27(5): p. 1133-1170.
- 5. Jomova, K., Alomar, S.Y., Nepovimova, E., Kuca, K. and Valko, M., 2025. Heavy metals: toxicity and human health effects. Archives of toxicology, 99(1), pp.153-209.
- 6. Oladimeji, T.E., Oyedemi, M., Emetere, M.E., Agboola, O., Adeoye, J.B. and Odunlami, O.A., 2024. Review on the impact of heavy metals from industrial wastewater effluent and removal technologies. Heliyon, 10(23).
- 7. Aziz, K.H.H., Mustafa, F.S., Omer, K.M., Hama, S., Hamarawf, R.F. and Rahman, K.O., 2023. Heavy metal pollution in the aquatic environment: efficient and low-cost removal approaches to eliminate their toxicity: a review. RSC advances, 13(26), pp.17595-17610.
- 8. Kahal, A., El-Sorogy, A.S., Qaysi, S., Almadani, S., Kassem, O.M. and Al-Dossari, A., 2020. Contamination and ecological risk assessment of the Red Sea coastal sediments, southwest Saudi Arabia. Marine pollution bulletin, 154, p.111125.
- 9. Wang, L.K., et al., Physicochemical treatment consisting of chemical coagulation, precipitation, sedimentation, and flotation. Integrated natural resources research, 2021: p. 265-397.
- 10. Amini, A., et al., Environmental and economic sustainability of ion exchange drinking water treatment for organics removal.

 Journal of Cleaner Production, 2015. 104: p. 413-421.
- 11. Liu, C., et al., Evaluating the efficiency of nanofiltration and reverse osmosis membrane processes for the removal of perand polyfluoroalkyl substances from water: A critical review. Separation and Purification Technology, 2022. 302: p. 122161.
- 12. Gupta, V.K., et al., A critical analysis on the efficiency of activated carbons from low-cost precursors for heavy metals remediation. Critical Reviews in Environmental Science and Technology, 2015. 45(6): p. 613-668.
- 13. Nawaz, S., et al., Effective assessment of biopolymer-based multifunctional sorbents for the remediation of environmentally hazardous contaminants from aqueous solutions. Chemosphere, 2023. 329: p. 138552.
- 14. Martău, G.A., M. Mihai, and D.C. Vodnar, The use of chitosan, alginate, and pectin in the biomedical and food sector—biocompatibility, bioadhesiveness, and biodegradability. Polymers, 2019. 11(11): p. 1837.
- 15. Dongre, R.S., Marine polysaccharides in pharmaceutical uses: chitin, chitosan, alginate, and carrageenan, in Polysaccharides of Microbial Origin: Biomedical Applications. 2021, Springer. p. 1-35.
- 16. Joseph, T.M., et al., Chemical modifications of alginate-based biopolymers, in Handbook of Natural Polymers, Volume 2. 2024, Elsevier. p. 97-122.
- 17. Cao, Y., et al., Specific binding of trivalent metal ions to λ-carrageenan. International journal of biological macromolecules, 2018. 109: p. 350-356.
- 18. Al-Fakeh, M.S.; Alazmi, M.S.; EL-Ghoul, Y. Preparation and Characterization of Nano-Sized Co(II), Cu(II), Mn(II) and Ni(II) Coordination PAA/Alginate Biopolymers and Study of Their Biological and Anticancer Performance. Crystals 2023, 13, 1148.
- 19. Szewczuk-Karpisz, K., et al., Simultaneous adsorption of Cu (II) ions and poly (acrylic acid) on the hybrid carbon-mineral nanocomposites with metallic elements. Journal of Hazardous Materials, 2021. 412: p. 125138.
- 20. Chen, M., et al., Recent advances in alginate-based hydrogels for the adsorption–desorption of heavy metal ions from water: A review. Separation and Purification Technology, 2024: p. 128265.
- 21. Awed, M., et al., Tosyl-carrageenan/alginate composite adsorbent for removal of Pb2+ ions from aqueous solutions. BMC chemistry, 2024. 18(1): p. 8.
- 22. An, N., et al., Detection of Cu 2+ in an aqueous solution based on CS/PAA-modified fiber-optic SPR sensor. IEEE Sensors Journal, 2025.
- 23. Kasaai, M.R. A review of several reported procedures to determine the degree of N-acetylation for chitin and chitosan using infrared spectroscopy. Carbohydr. Polym. 2008, 71, 497–508.
- 24. Rochas, C.; Lahaye, M.; Yaphe, W. Sulfate Content of Carrageenan and Agar Determined by Infrared Spectroscopy. Bot. Mar. 1986, 29, 335–340.
- 25. EL-Ghoul, Y.; Al-Fakeh, M.S.; Al-Subaie, N.S. Synthesis and Characterization of a New Alginate/Carrageenan Crosslinked Biopolymer and Study of the Antibacterial, Antioxidant, and Anticancer Performance of Its Mn(II), Fe(III), Ni(II), and Cu(II) Polymeric Complexes. Polymers 2023, 15, 2511.
- 26. Chen, Y.; Sheng, Q.; Hong, Y.; Lan, M. Hydrophilic nanocomposite functionalized by carrageenan for the specific enrichment of glycopeptides. Anal. Chem. 2019, 91, 4047–4054.
- 27. EL-Ghoul, Y.; Alsamani, S. Highly Efficient Biosorption of Cationic Dyes via Biopolymeric Adsorbent-Material-Based Pectin Extract Polysaccharide and Carrageenan Grafted to Cellulosic Nonwoven Textile. Polymers 2024.

28. EL-Ghoul, Y.; Ammar, C.; Alminderej, F.M.; Shafiquzzaman, M. Design and Evaluation of a New Natural Multi-Layered Biopolymeric Adsorbent System-Based Chitosan/Cellulosic Nonwoven Material for the Biosorption of Industrial Textile Effluents. Polymers 2021, 13, 322.

- 29. Ammar, C., El Ghoul, Y. and El Achari, A., 2015. Finishing of polypropylene fibers with cyclodextrins and polyacrylic acid as a crosslinking agent. Textile Research Journal, 85(2), pp.171-179.
- 30. Rajapaksha, A.U., et al., A systematic review on adsorptive removal of hexavalent chromium from aqueous solutions: Recent advances. Science of the Total Environment, 2022. 809: p. 152055.
- 31. El-Badry, B., et al., Efficacy of mesoporous TiO2–ZrO2@ g-C3N4 produced using a simple ultrasonic approach for copper ion removal from wastewater. Journal of Science: Advanced Materials and Devices, 2024. 9(4): p. 100772.
- 32. Blesa, M.A., et al., The interaction of metal oxide surfaces with complexing agents dissolved in water. Coordination Chemistry Reviews, 2000. 196(1): p. 31-63.
- 33. Younis, A.M., et al., Enteromorpha compressa Macroalgal Biomass Nanoparticles as Eco-Friendly Biosorbents for the Efficient Removal of Harmful Metals from Aqueous Solutions. Analytica, 2024. 5(3): p. 322-342.
- 34. Liu, L., et al., Distinct chromium removal mechanisms by iron-modified biochar under varying pH: Role of iron and chromium speciation. Chemosphere, 2023. 331: p. 138796.
- 35. El-Khateeb, M.A., Nashy, E.L., Saad, A. and Ali, F.A., 2025. Synthesized Meso AC & Fenton oxidation for Copper Removal & environment impact of Electroplating wastewater, Kinetic Study. Egyptian Journal of Chemistry, 68(7), pp.351-364
- 36. Wiśniewska, M., et al., Comparison of adsorption affinity of anionic and cationic polyacrylamides for montmorillonite surface in the presence of chromium (VI) ions. Adsorption, 2019. 25: p. 41-50.
- 37. Younis, A.M., E.M. Elkady, and M. El-Naggar, Biosorption of Arsenic (III) and Arsenic (V) from Aqueous Solutions: Equilibrium and Kinetic Studies using Mangrove Leaf Biomass (Avicennia marina). Egyptian Journal of Aquatic Biology & Fisheries, 2023. 27(6).
- 38. Singha, S., U. Sarkar, and P. Luharuka, Functionalized granular activated carbon and surface complexation with chromates and bi-chromates in wastewater. Science of the total environment, 2013. 447: p. 472-487.
- 39. Hoang, A.T., et al., Remediation of heavy metal polluted waters using activated carbon from lignocellulosic biomass: An update of recent trends. Chemosphere, 2022. 302: p. 134825.
- 40. Lin, S., et al., Study on competitive adsorption mechanism among oxyacid-type heavy metals in co-existing system: Removal of aqueous As (V), Cr (III) and As (III) using magnetic iron oxide nanoparticles (MIONPs) as adsorbents. Applied Surface Science, 2017. 422: p. 675-681.
- 41. Donati, I. and B.E. Christensen, Alginate-metal cation interactions: Macromolecular approach. Carbohydrate polymers, 2023. 321: p. 121280.
- 42. Deze, E.G., et al., Porous alginate aerogel beads for effective and rapid heavy metal sorption from aqueous solutions: Effect of porosity in Cu2+ and Cd2+ ion sorption. Chemical engineering journal, 2012. 209: p. 537-546.
- 43. Liu, W., et al., Adsorption of Pb2+, Cd2+, Cu2+ and Cr3+ onto titanate nanotubes: Competition and effect of inorganic ions. Science of the Total Environment, 2013. 456: p. 171-180.
- 44. Bakatula, E., et al., Biosorption of trace elements from aqueous systems in gold mining sites by the filamentous green algae (Oedogonium sp.). Journal of Geochemical Exploration, 2014. 144: p. 492-503.
- 45. Naskar, A. and D. Bera, Mechanistic exploration of Ni (II) removal by immobilized bacterial biomass and interactive influence of coexisting surfactants. Environmental Progress & Sustainable Energy, 2018. 37(1): p. 342-354.
- 46. Awual, M.R., et al., pH dependent Cu (II) and Pd (II) ions detection and removal from aqueous media by an efficient mesoporous adsorbent. Chemical Engineering Journal, 2014. 236: p. 100-109.
- 47. Acharya, R., A. Lenka, and K. Parida, Magnetite modified amino group based polymer nanocomposites towards efficient adsorptive detoxification of aqueous Cr (VI): A review. Journal of Molecular Liquids, 2021. 337: p. 116487.
- 48. Molina, M., K. Manquian-Cerda, and M. Escudey, Sorption and selectivity sequences of Cd, Cu, Ni, Pb, and Zn in singleand multi-component systems in a cultivated Chilean Mollisol. Soil and Sediment Contamination, 2010. 19(4): p. 405-418.
- 49. Li, Z., Lu, G., Du, D. and Zhao, D., 2025. Harnessing low-cost adsorbents for removal of heavy metals and metalloids in contaminated water: Progress in the past decade and future perspectives. Journal of Cleaner Production, p.145845.
- 50. Kavand, M., et al., Film-pore-[concentration-dependent] surface diffusion model for heavy metal ions adsorption: single and multi-component systems. Process Safety and Environmental Protection, 2017. 107: p. 486-497.
- 51. Efome, J.E., et al., Insight studies on metal-organic framework nanofibrous membrane adsorption and activation for heavy metal ions removal from aqueous solution. ACS applied materials & interfaces, 2018. 10(22): p. 18619-18629.
- 52. Serrano, S., et al., A surface complexation and ion exchange model of Pb and Cd competitive sorption on natural soils. Geochimica et Cosmochimica Acta, 2009. 73(3): p. 543-558.
- 53. Pei Gan, P. and S.F. Yau Li, Biosorption of elements. 2013.
- 54. Lun, L., et al., Co-adsorption and competitive adsorption of sulfamethoxazole by carboxyl-rich functionalized corn stalk cellulose in the presence of heavy metals. Industrial Crops and Products, 2023. 199: p. 116761.